I&EC research
Industrial & Engineering Chemistry Research

pubs.acs.org/IECR

Article

Investigation of the Antisolvent Effect on the Phase Behavior of Amino Acid Solid Solutions

Vico Tenberg, Mahsa Hokmabadi, Andreas Seidel-Morgenstern, Heike Lorenz, and Masoud Sadeghi*

Cite This: *Ind. Eng. Chem. Res.* 2023, 62, 753−761

Read Online

ACCESS | Metrics & More | Article Recommendations | Supporting Information

ABSTRACT: This work focuses on the experimental measurement and modeling of solid−liquid equilibria containing continuous binary solid solutions crystallized from solvent mixtures for the usage in antisolvent crystallization. The newly constructed quaternary phase diagrams of L-valine/L-leucine in water/2-propanol and water/acetone systems are analyzed and compared to those of water/ethanol mixtures. Experimental data sets are determined via high-performance liquid chromatography, while the formation of solid solutions is confirmed with powder X-ray diffraction. Our validated modeling approach for the ternary L-valine/L-leucine/water mixture is extended to the aforementioned quaternary systems. The modeling combines the Perturbed Chain-Statistical Associating Fluid Theory and the Non-Random Two-Liquid model to describe the liquid and solid phases, respectively. Additionally, two modeling approaches (predictive and semi-predictive) are proposed. Both models show good agreement with the experimental solubility data sets of the binary solutions. However, larger deviations were observed in three- and four-component systems, especially toward the solubility maxima. Therefore, the modeling approach should be used for qualitative initial antisolvent screenings for the separation of solid solutions using counter-current crystallization.

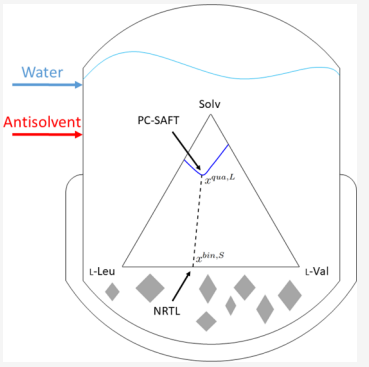

1. INTRODUCTION

Crystallization is a widely utilized unit operation for the purification and solid phase design of target products. To efficiently design crystallization processes, knowledge of the solid−liquid equilibria (SLE) of the desired compounds is required. This holds true especially if more complex solid phase behaviors such as the formation of solid solutions are present. Here, two or more compounds show continuous or partial miscibility in the solid phase.[1] For solid solution-forming systems, the solubilities of the compounds and their crystallization behavior are important. Solid solutions crystallize along the tie lines and therefore, a stepwise purification is required for enrichment in the specific phases. This can be utilized in counter-current crystallization to effectively separate solid solutions.[2−6]

In this regard, systems of solid solution-forming salts were studied incorporating mass balances in an empirical model to simulate the counter-current crystallization process.[2] Moreover, evaporative and antisolvent crystallizations were coupled to bypass the alyotropic point in the amino acid solid solutions.[3] Complex phase behaviors imply extensive experimental effort in order to reliably gain insights into the system. Thermodynamic modeling approaches can decrease the amount of experimental work by calculating missing data sets. In addition, they are important to gain a qualitative knowledge of the phase behavior of the system with minimal experimental effort. Moreover, they may help the practitioner during the solvent selection process. This is especially helpful if we face multicomponent multiphase equilibria such as the SLE behavior of the amino acids in mixed solvents. In the literature, several publications are available, which focus on amino acid solubility determination.[7−9] These values are obtained in aqueous[8,9] as well as non-aqueous[7] solutions at different temperatures. Moreover, the effect of nonidealities were considered using thermodynamic models.[8,9] Additionally, a few studies determined amino acid solubilities in mixed solvents.[10−12] Specifically, L-valine solubility was measured in mixed solvent systems,[10] and also the solubility of other amino acids in mixed alcohol−water solutions was reported and modeled.[11,12] They also used thermodynamic models to represent the solubility lowering of amino acids due to the addition of alcohols in water.[12] Solubilities of amino acid mixtures were previously reported in refs 3, 13−19. Formation of solid solutions in some amino acid systems,[13,14] the mutual effect of amino acids on each other's solubility,[16] and the purity of amino acid crystals[19] were studied in detail. However, in some cases,[16] the formation of solid solutions in the L-valine/L-leucine system, validated in, for example, refs13 and 14, was not regarded. SAFT-based as well as local composition models are widely used to model amino acid SLE behavior, for example, refs 8, 9, and 16. In most of the amino acid-related studies, the solid

Received: August 30, 2022
Revised: December 10, 2022
Accepted: December 13, 2022
Published: December 22, 2022

phase was pure; thus, solid phase non-ideality and purity were not taken in to account. However, there are few studies regarding the solid solution formation in some amino acid systems,[3,13−15,17−19] and modeling approaches to account for the formation of solid solutions are given in the respective literature.[13,19]

Evaporative crystallization is a widely used technique for the purification of mixed crystals.[2,4,5,20] In isothermal evaporative crystallization, complex phase behaviors like alyotropes can limit the resolutions of solid solutions. Additionally, due to heat transfer limitation, crystal growth is slow, which generally results in larger crystal size distributions. In such cases, antisolvent crystallization provides a flexible, although more complex, alternative to evaporative crystallization; regardless of the chosen method, it is important to know the phase diagram of the solvent/mixed crystal system to properly describe such a process. Hence, we previously combined Perturbed Chain-Statistical Associating Fluid Theory (PC-SAFT)[21] with Non-Random Two-Liquid (NRTL)[22] to model SLE of L-valine/L-leucine solid solution mixtures in water.[13] To reduce the high energy demand of water evaporation, antisolvent crystallization was utilized alongside evaporative crystallization to improve the separation efficiency of solid solutions.[3] As a prerequisite, we need to describe the phase diagrams in the presence of different antisolvents.

In this work, different new SLE data sets for L-valine/L-leucine in aqueous solutions of 2-propanol or acetone were measured. Based on these data sets, phase diagrams are constructed at various temperatures. Second, our previous modeling method is extended to be applicable for quaternary systems including solvent mixtures and binary continuous solid solutions. Finally, two alternative approaches for the construction of phase diagrams based on recently reported melting data[23] or binary solubilities are proposed and validated.

2. EXPERIMENTAL PART

2.1. Chemicals. The following chemicals were used in this work: L-valine (CAS: 72-18-4, Iris Biotech GmbH), L-leucine (CAS: 61-90-5, Iris Biotech GmbH), ethanol (CAS: 64-17-5, VWR International), 2-propanol (CAS: 67-63-0, VWR International), acetone (CAS: 67-64-1, VWR International), and water. The water was deionized with a Millipore 40 filter [resistivity: 18.2 MΩ cm, total organic carbon (TOC): 3 ppb] while the other compounds were used as received without further purification. Additional information about the chemicals is shown in Table 1.

2.2. Solubility Determination and Solid Phase Analysis. Binary solubility measurements of L-leucine in the organic solvents were performed as follows. An excess of L-leucine was given to a specific solvent, the vial was sealed, and it was stirred at a constant temperature for at least 24 h. After this dissolution period, the liquid phase was sampled and analyzed by high-performance liquid chromatography (HPLC). For the measurement of ternary solubility data, various mixtures of L-valine and L-leucine were dissolved in water. Upon reaching complete dissolution, specific amounts of the organic solvent, acting as an antisolvent, were added and the vials were sealed. The vials were kept at a constant temperature and stirred continuously for at least 72 h to reach equilibrium. Then, the liquid phase was sampled with a syringe and a syringe filter (pore size: 0.45 μm) after which the remaining solid and liquid phases were separated via filtration and the solid phase was sampled from the filter cake. Both phases were analyzed by HPLC. For this, the samples were diluted in a 2 mmol copper sulfate/methanol (90/10 vol %) eluent solution and injected in volumes of 3 μL and a flow rate of 0.5 mL min^{-1}. A Phenomenex Chirex 3126 (D)-penicillamine column (length 50 mm, diameter 4.6 mm) was used for the separation of the amino acids. Due to the UV-activity of acetone, for samples containing acetone, an identical but longer column (length: 250 mm, diameter 4.6 mm) with an injection volume of 30 μL and a flow rate of 0.5 mL min^{-1} was used. The concentrations of the amino acids were calculated with predetermined calibration lines. The solid phase was additionally analyzed via powder X-ray diffraction (PXRD) to validate solid solution formation. The measurements were performed with a PANalytical X'Pert Pro diffractometer using $Cu_{K\alpha}$ radiation within a 2θ range between 4 and 32° and a step size of 0.0167° where each step was measured for 200 s.

Table 1. Chemicals Used in This Work

chemical	CAS	purity	supplier	molar mass [g/mol]
L-valine	72-18-4	98.8% (Assay)	Iris Biotech GmbH	117.15
L-leucine	61-90-5	100.3% (Assay)	Iris Biotech GmbH	131.17
ethanol	64-17-5	>99.7%	VWR International	46.07
2-propanol	67-63-0	>99.8%	VWR International	60.10
acetone	67-64-1	>99.8%	VWR International	58.08

3. THEORY

At thermodynamic equilibrium, the chemical potential of the solute i in the liquid phase is equal to its chemical potential in the solid phase. Following,[24] this can be described in terms of the activity of the solute in the liquid and the ratio of standard-state fugacities

$$\ln\left(\frac{f_i^{0,S}}{f_i^{0,L}}\right) = \ln(a_{i,\text{solute}}) = \ln(x_i\gamma_i) \tag{1}$$

where $f_i^{0,S}$ is the fugacity of pure solid i, $f_i^{0,L}$ is the fugacity of pure i as a subcooled liquid, x_i is the molar fraction, and γ_i is the activity coefficient of component i in the liquid phase with respect to the pure subcooled liquid i at the system temperature as the standard state. Considering a pure solid, the ratio of standard-state fugacities can be calculated using thermoanalytical measurements such as melting temperature $T_{m,i}$, molar melting enthalpy $\Delta H_{m,i}$, and temperature-dependent molar heat capacity difference between the pure solid and its melt $\Delta C_{p,m,i}(T)$

$$\ln\left(\frac{f_i^{0,S}}{f_i^{0,L}}\right) = -\frac{\Delta H_{m,i}(T_{m,i})}{RT}\left(1 - \frac{T}{T_{m,i}}\right) - \frac{1}{RT}\int_{T_{m,i}}^{T}\Delta C_{p,m,i}(T)\,dT + \frac{1}{R}\int_{T_{m,i}}^{T}\frac{\Delta C_{p,m,i}(T)}{T}\,dT \tag{2}$$

R and T are the gas constant and temperature, respectively. In this work, $\Delta C_{p,m,i}(T)$ is calculated using a linear temperature-dependent approach given in ref 8.

https://doi.org/10.1021/acs.iecr.2c03122
Ind. Eng. Chem. Res. 2023, 62, 753−761

$$\Delta C_{p,m,i}(T) = (a^{L}_{p,m,i} - a^{S}_{p,m,i})T + (b^{L}_{p,m,i} - b^{S}_{p,m,i}) \quad (3)$$

where $a^{L}_{p,m,i}$, $a^{S}_{p,m,i}$ and $b^{L}_{p,m,i}$, $b^{S}_{p,m,i}$ are constants that describe the temperature dependence of $\Delta C_{p,m,i}(T)$ and are given in the Supporting Information.

For ternary liquid mixtures in equilibrium with a binary solid solution, the iso-fugacity criterion using the standard-state fugacities f_i^0 reads

$$x_i^{bin,S}\gamma_i^{bin,S}f_i^{0,S} = x_i^{ter,L}\gamma_i^{ter,L}f_i^{0,L} \quad (4)$$

with bin and ter denoting a binary and ternary and L and S a liquid phase and a solid phase, respectively. The ratio of standard-state fugacities may be calculated using eq 2 with the help of thermoanalytical data. Although amino acids decompose before they melt, recently, fast scanning calorimeters are used to obtain their melting data.[23] Alternatively, the standard-state fugacity ratio can be related to the solubility data for a pure solid in equilibrium with its solution in a solvent

$$f_i^{0,S} = x_i^{bin,L}\gamma_i^{bin,L}f_i^{0,L} \quad (5)$$

A combination of eqs 1, 2, and 5 for a set temperature results in a constant activity regardless of the solvent and solvent composition. Combining eqs 4 and 5 leads to an equation describing the relation of the activity coefficients and solubilities in a system of solid solution forming solutes i in equilibrium with a corresponding liquid phase.

$$x_i^{bin,S}\gamma_i^{bin,S} = \frac{x_i^{ter,L}\gamma_i^{ter,L}}{x_i^{bin,L}\gamma_i^{bin,L}} \quad (6)$$

This approach was already used to model the solid solution phase behavior of the L-valine/L-leucine/water system.[13]

Equation 6 is easily extended for more complex systems following the same approach. For a quaternary (qua) system containing an equilibrium between a binary solid solution and a quaternary liquid phase, the following equation is derived

$$x_i^{bin,S}\gamma_i^{bin,S} = \frac{x_i^{qua,L}\gamma_i^{qua,L}}{x_i^{ter,L}\gamma_i^{ter,L}} \quad (7)$$

In this work, the liquid phase activity coefficients are calculated using the PC-SAFT equation of state (EoS) while the solid phase activity coefficients are determined by using the NRTL model. It is noted that even though amino acids are prone to exist as zwitterions, this work considers them as neutral molecules with regard to the modeling. Both models are described in the following sections.

3.1. Perturbed Chain-Statistical Associating Fluid Theory Equation of State. In the PC-SAFT EoS, molecules are considered as chains of interconnected spheres. These chains impose various interactions with other chains of the same type or different chains describing a different molecule. To represent these chains mathematically, three distinct parameters are used: the number of segments m in the chain, the diameter of one segment σ, and the dispersion energy imposed by the chain u/k. For components which are capable to form hydrogen bonds, two more parameters are needed to describe these associating properties. These parameters are the association energy $\frac{\varepsilon^{A_iB_i}}{k}$ and the association volume $\kappa^{A_iB_i}$. Therefore, five component-specific parameters are needed to describe a compound. With them, the compressibility factor Z is determined as the sum of the contributions imposed by the chain.[25]

$$Z = 1 + Z^{hc} + Z^{disp} + Z^{assoc} \quad (8)$$

Derivation and equations for the hard chain Z^{hc} and dispersion Z^{disp} contributions are found in ref 21, while the association Z^{assoc} contribution is given in ref 26. For mixed systems, the following mixing rules are applied[21,25]

$$\left(\frac{u}{k}\right)_{ij} = (1 - k_{ij})\sqrt{\left(\frac{u}{k}\right)_{ii}\left(\frac{u}{k}\right)_{jj}} \quad (9)$$

$$\sigma_{ij} = \frac{1}{2}(\sigma_i + \sigma_j) \quad (10)$$

$$\frac{\varepsilon^{A_iB_j}}{k} = \frac{1}{2}\left(\frac{\varepsilon^{A_iB_i}}{k} + \frac{\varepsilon^{A_jB_j}}{k}\right) \quad (11)$$

$$\kappa^{A_iB_j} = \left(\frac{\sqrt{\sigma_i\sigma_j}}{\sigma_{ij}}\right)^3\sqrt{\kappa^{A_iB_i}\kappa^{A_jB_j}} \quad (12)$$

k_{ij} is used to correct the geometric mean assumption in the dispersion energy in eq 9. This parameter is usually fitted to binary experimental data using the following equation[23]

$$k_{ij} = k_{ij,T_0} + k_{ij,T}\cdot(T - T_0) \quad (13)$$

3.2. NRTL Model. The NRTL model offers a simple temperature-dependent, semi-empirical determination of the activity coefficient. In this work, it is used to calculate the activity coefficients of the binary solid phase of the solid solution forming amino acids. For a mixture of A and B, the NRTL model is given in ref 22 as follows

$$\ln(\gamma_B) = x_A^2\left[\tau_{AB}\left(\frac{g_{AB}}{x_B + x_A g_{AB}}\right)^2 + \frac{g_{BA}\tau_{BA}}{(x_A + x_B g_{BA})^2}\right] \quad (14)$$

with

$$g_{AB} = \exp(-\alpha\tau_{AB}) \quad (15)$$

$$g_{BA} = \exp(-\alpha\tau_{BA}) \quad (16)$$

$$\tau_{AB} = \frac{b_{AB}}{RT} \quad (17)$$

$$\tau_{BA} = \frac{b_{BA}}{RT} \quad (18)$$

The parameters b_{AB} and b_{BA} as well as the non-randomness parameter α are determined by adjusting them to the experimental data.

4. RESULTS AND DISCUSSION

4.1. Solubility Measurements. In this work, several solubilities for L-leucine in various organic solvents and for L-leucine/L-valine mixtures in water/isopropanol and water/acetone mixtures are presented. The pure solubility data for L-valine, used later in this work, were published in ref 7. Similarly, solubilities of L-leucine/L-valine mixtures at 25 °C in water and water/ethanol mixtures were published in our previous works[13] and ref 3, respectively. The measured solubilities of pure L-leucine are shown in Table 2.

The formation of solid solutions of the L-leucine/L-valine system crystallized from water and water/ethanol mixtures has already been validated by PXRD in our previous works.[3,13] This

https://doi.org/10.1021/acs.iecr.2c03122
Ind. Eng. Chem. Res. 2023, 62, 753−761

Table 2. Solubilities of L-Leucine in Various Solvents from 298.35 to 337.95 K[a]

	$x_{\text{L-leu,L}} \cdot 10^{-4}$		
T [K]	ethanol	2-propanol	acetone
298.35	0.7484	0.1362	0.7567
308.35	0.8771	0.1779	1.1912
318.35	1.0864	0.2203	1.8479
327.95	1.3456	0.2905	
337.95	1.6174	0.3485	

[a]Standard uncertainties are $u(T) = 0.2$ K and $U(x_L) \leq 1.45 \times 10^{-6}$ for ethanol, $U(x_L) \leq 7.07 \times 10^{-7}$ for 2-propanol, and $U(x_L) \leq 2.55 \times 10^{-6}$ for acetone (for a 0.95 level of confidence).

work extends this for crystals obtained from water/2-propanol and water/acetone solutions. Figure 1 shows the selected PXRD patterns for these systems. Most notably, a continuous gradual shift of the main peak (6−8°) is observed. Additionally, the patterns show a single-phasic behavior, which confirms the solid solution formation. The only exceptions to this are the two samples containing 7.06 mol % L-valine in the 2-propanol-containing and 40.12 mol % L-valine in the acetone-containing solvent mixtures, where two phases can be observed (e.g., in the 2θ range between 6 and 8°). However, this can be attributed to a non-complete equilibration and the formation of a meta-stable co-crystal V_3L,[27] respectively.

In Figure 2, acetone shows the lowest solubility for L-valine, while ethanol shows the highest solubility of the discussed solvents. This can be attributed to the polarity and the ability to form hydrogen bonds, which favors the dissolution of L-valine in ethanol.

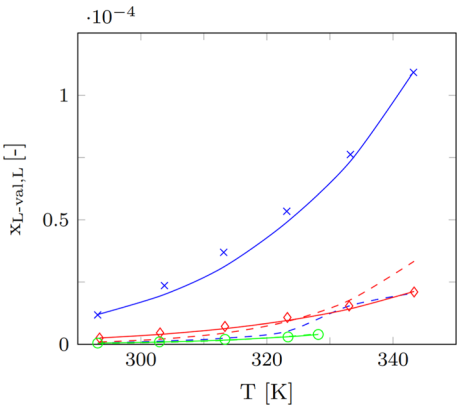

Figure 2. Solubilities of L-valine in ethanol (blue, ×), 2-propanol (red, ◊), and acetone (green, ○) between 293.15 and 343.35 K. Dots are experimental data points from ref 7, and lines are calculated using PC-SAFT (solid lines with fitted k_{ij} and dashed lines with $k_{ij} = 0$).

However, as presented in Table 2 and Figure 3, acetone results in the highest while 2-propanol exhibits the lowest solubility and solubility temperature dependency for L-leucine out of the measured solvents in this work. Due to the larger and less polar structure of L-leucine, the influence of the hydrogen bonds on the solubility is reduced and less polar solvents such as acetone are more suited as solvents.

In addition to the diffractograms in Figure 1, Tables 3 and 4 show measured solubility data for mixed L-valine/L-leucine systems at 298.15 K. These data sets form the basis for comparison with the modeled solubilities and tie line behavior in the next chapter.

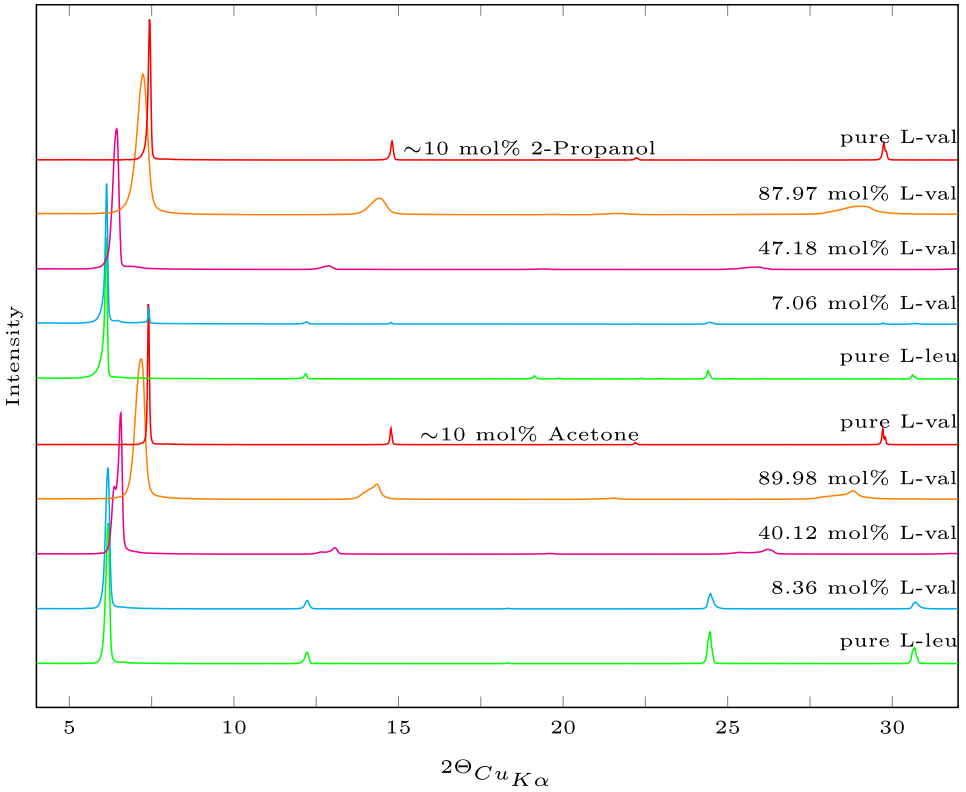

Figure 1. Selected PXRD patterns of crystals obtained from L-valine/L-leucine/water solutions containing roughly 10 mol % of 2-propanol or acetone as the antisolvent.

https://doi.org/10.1021/acs.iecr.2c03122
Ind. Eng. Chem. Res. 2023, 62, 753−761

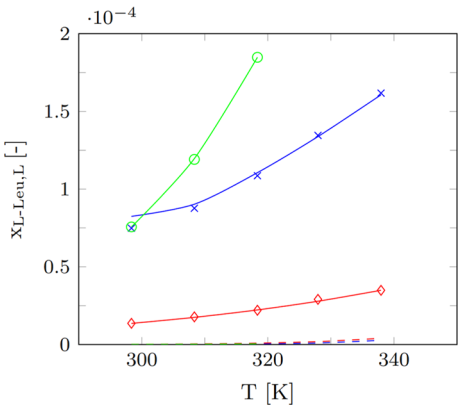

Figure 3. Solubilities of L-leucine in ethanol (blue, ×), 2-propanol (red, ◊), and acetone (green, ○) between 298.35 and 337.95 K. Dots are experimental data points (see Table 2) and lines are calculated using PC-SAFT (solid lines with fitted k_{ij} and dashed lines with $k_{ij} = 0$).

Table 3. Liquid and Solid Phase Equilibrium Data for L-Valine/L-Leucine in Various Water/2-Propanol Mixtures at 298.15 K[a]

$x_{L\text{-val,L}}$	$x_{L\text{-leu,L}}$	$x_{IPA,L}$	$x_{L\text{-val,S}}$	$x_{L\text{-leu,S}}$
0.0048	0.0000	0.0900	1.00	0.00
0.0060	0.0006	0.0903	0.92	0.08
0.0065	0.0008	0.0910	0.88	0.12
0.0065	0.0010	0.0901	0.83	0.17
0.0068	0.0014	0.0905	0.47	0.53
0.0047	0.0017	0.0907	0.27	0.73
0.0022	0.0019	0.0907	0.07	0.93
0.0008	0.0018	0.0910	0.04	0.96
0.0000	0.0018	0.0912	0.00	1.00
0.0034	0.0000	0.1641	1.00	0.00
0.0047	0.0006	0.1655	0.91	0.09
0.0046	0.0006	0.1650	0.90	0.10
0.0048	0.0008	0.1651	0.84	0.16
0.0048	0.0012	0.1652	0.73	0.27
0.0040	0.0015	0.1650	0.38	0.62
0.0020	0.0018	0.1657	0.14	0.86
0.0007	0.0017	0.1658	0.06	0.95
0.0000	0.0017	0.1662	0.00	1.00
0.0027	0.0000	0.2310	1.00	0.00
0.0035	0.0005	0.2315	0.93	0.07
0.0037	0.0005	0.2293	0.91	0.09
0.0039	0.0007	0.2288	0.86	0.14
0.0041	0.0011	0.2290	0.76	0.24
0.0037	0.0014	0.2293	0.41	0.59
0.0020	0.0017	0.2298	0.14	0.86
0.0008	0.0017	0.2311	0.08	0.92
0.0000	0.0016	0.2339	0.00	1.00

[a]Standard uncertainties are $u(T) = 0.2$ K, $U(x_L) \leq 0.0004$, and $U(x_S) \leq 0.03$ (for a 0.95 level of confidence).

Both systems show an overall decrease in the solubility with an increase of the antisolvent fraction. Additionally, the solubility of L-leucine is between two and five times lower than the solubility of L-valine depending on the solvent composition. All measured data sets also show an increase in the solubility of L-valine/L-leucine mixtures over the pure solubilities. This "salting-in" behavior was observed for these amino acids in water and water/ethanol mixtures as well.[3,13] Following Tables 3 and 4, all these systems show an alyotropic behavior.[28] The solubility decrease, due to antisolvent addition, behaves similarly for ethanol and 2-propanol, while acetone has a stronger antisolvent effect and thus decreases the solubility further per fraction of antisolvent in the solvent phase.

Table 4. Liquid and Solid Phase Equilibrium Data for L-Valine/L-Leucine in Various Water/Acetone Mixtures at 298.15 K[a]

$x_{L\text{-val,L}}$	$x_{L\text{-leu,L}}$	$x_{Ace,L}$	$x_{L\text{-val,S}}$	$x_{L\text{-leu,S}}$
0.0059	0.0000	0.0899	1.00	0.00
0.0073	0.0007	0.0894	0.94	0.07
0.0078	0.0010	0.0900	0.90	0.10
0.0080	0.0014	0.0897	0.81	0.19
0.0070	0.0016	0.0896	0.40	0.60
0.0054	0.0024	0.0896	0.22	0.78
0.0025	0.0024	0.0906	0.08	0.92
0.0009	0.0023	0.0902	0.03	0.98
0.0000	0.0023	0.0907	0.00	1.00
0.0045	0.0000	0.1062	1.00	0.00
0.0054	0.0006	0.1090	0.94	0.06
0.0056	0.0009	0.1115	0.88	0.12
0.0057	0.0010	0.1118	0.84	0.16
0.0058	0.0013	0.1109	0.65	0.35
0.0048	0.0016	0.1098	0.36	0.64
0.0023	0.0017	0.1120	0.09	0.91
0.0009	0.0017	0.1127	0.04	0.96
0.0000	0.0016	0.1132	0.00	1.00
0.0039	0.0000	0.1290	1.00	0.00
0.0044	0.0005	0.1280	0.92	0.06
0.0049	0.0007	0.1309	0.90	0.11
0.0051	0.0009	0.1286	0.85	0.15
0.0050	0.0011	0.1299	0.72	0.28
0.0045	0.0014	0.1292	0.40	0.60
0.0023	0.0016	0.1282	0.10	0.90
0.0008	0.0009	0.1297	0.004	0.996
0.0000	0.0008	0.1306	0.00	1.00

[a]Standard uncertainties are $u(T) = 0.2$ K, $U(x_L) \leq 0.0002$, and $U(x_S) \leq 0.01$ (for a 0.95 level of confidence).

4.2. SLE Modeling. An approach for the modeling of continuous solid solutions was presented in a previous work.[13] This approach used a combination of NRTL and PC-SAFT modeling to calculate the activity coefficients for the solid and liquid phases, respectively (see eq 6). In this work, this approach is extended for quaternary mixtures for the application of antisolvent crystallization for the separation of solid solutions. For the calculation of the liquid phase activity coefficients using PC-SAFT, the component-specific parameters and the binary interaction parameter k_{ij} are required. The component-specific parameters, the melting properties of the amino acids, as well as the interactions of all compounds with water can be found in the literature[8,29,30] (see the Supporting Information), while our previous work verified that fitting the interaction between L-valine and L-leucine did not improve the accuracy of the model.[13] Therefore, in this work, $k_{L\text{-val/L-leu}} = 0$ is used. To the best of our knowledge, at the time of writing, no interaction parameters, based on PC-SAFT, between the amino acids and the antisolvents are available in literature and thus are fitted to binary solubility data in this work, which are listed in the Supporting Information as well. Altogether, six k_{ij,T_0} and six $k_{ij,T}$ were fitted in this work, one each to all of the possible combinations of the two amino acids and the three antisolvents.

https://doi.org/10.1021/acs.iecr.2c03122
Ind. Eng. Chem. Res. 2023, 62, 753−761

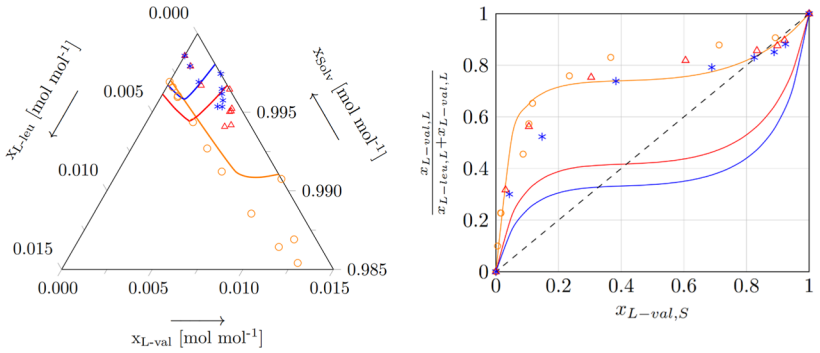

Figure 4. Left: Ternary phase diagram; right: distribution diagram of L-valine/L-leucine in water (orange, ○). 16 mol % ethanol/water (red, Δ) and 23.1 mol % ethanol/water (blue, *) at 298.15 K. The solid lines are calculated with eq 7 using melting data. Experimental data acquired from refs 6 and 7.

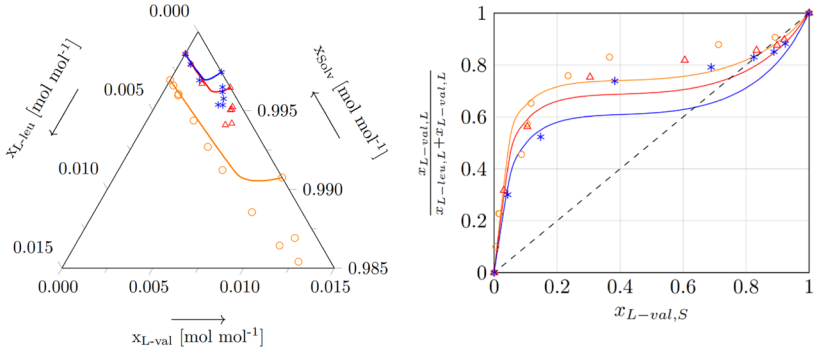

Figure 5. Left: Ternary phase diagram; right: distribution diagram of L-valine/L-leucine in water (orange, ○). 16 mol % ethanol/water (red, Δ) and 23.1 mol % ethanol/water (blue, *) at 298.15 K. The solid lines are calculated with eq 7 using experimental (pseudo-)binary solubility data. Experimental data acquired from refs 3 and 13.

For fitting the k_{ij} parameters to the solubility data of either amino acid in each solvent, using eq 1, pure component parameters and melting data given in Tables S1 and S2 in the Supporting Information were used. However, only the highest and lowest temperatures were considered in the fitting while the solubilities at the temperatures in-between were predicted. The resulting k_{ij} parameters are given in Table S3. Figure 2 shows the solubility data for pure L-valine, gathered from ref 7, while L-leucine solubilities, measured in this work, are shown in Figure 3. As it can be seen in these figures, the model is in good agreement with the experimental data sets and therefore, the determined parameters, for 298.15 K, are used in further modeling of the solid solution SLE behavior. However, the results with $k_{ij} = 0$ (see the dashed lines in Figures 2 and 3) show that the model has difficulties in distinguishing between different solvents for these solutes. With $k_{ij} = 0$, 2-propanol shows higher solubilities for L-valine than ethanol, while acetone can be described very well since it almost matches the fitted line. In the case of L-leucine, with $k_{ij} = 0$, the model underestimates the solubilities substantially and cannot distinguish between the solvents used.

For the modeling of solid solution behavior using eq 7, a description for the solid phase activity coefficients is needed. In this work, these coefficients are calculated using the NRTL model. In a previous work, its parameters were fitted to ternary equilibrium data of L-valine and L-leucine in water at 298.15 K,[13] which are given in the Supporting Information.

Figure 4 shows the ternary phase diagram (left) and tie line behavior in a Roozeboom distribution diagram (right) for L-valine and L-leucine in various water/ethanol mixtures at 298.15 K. Roozeboom diagrams plot the solvent-free liquid fraction of the solutes over its corresponding solid phase equilibrium composition and are a valuable tool in the design of countercurrent crystallization.[2,3,31] Here, melting data were used to calculate the ratio of standard state fugacities and therefore, with eq 1, the activity of the solute in the liquid phase. The solubility of the amino acids in water is in good agreement with the experimental data toward the edges of the ternary phase diagram; however, the accuracy decreases toward the solubility maximum. It can be seen that the solubility decrease due to the ethanol addition can be modeled reasonably well for L-valine; however, the model shows an increase for L-leucine, which is not shown by the experimental data. However, here, we would like to emphasize the scaling of the diagram in Figure 4 (left). Since the solubilities are relatively low for these compounds, the absolute error is reasonably small regardless of the elevated relative error. Further, the model is capable of showing alyotropic behavior for all data sets as well as the qualitatively correct trend for the alyotrope shift. However, quantitatively, the model accuracy is rather low; hence, the model might not be suited for reliable antisolvent screenings. We found that the model is not able to produce accurate data with a fixed ratio of standard state fugacities, which in reality is a constant value independent of the solvent phase composition (eq 1). In this work, we propose an additional, semi-predictive alternative to this modeling approach.

This approach uses experimental solubility data (see eq 5) of a solute in the specific solvent or solvent mixture as a constant parameter for the model, while its corresponding activity coefficient is calculated by PC-SAFT. This allows the (pseudo-)binary liquid activity to change with the solvent composition

https://doi.org/10.1021/acs.iecr.2c03122
Ind. Eng. Chem. Res. 2023, 62, 753−761

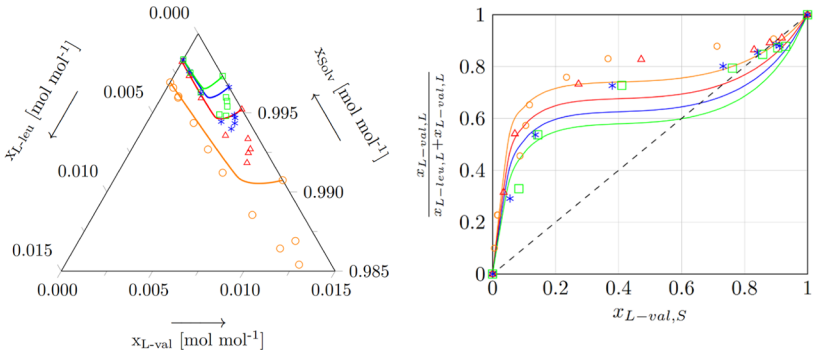

Figure 6. Left: Ternary phase diagram; right: distribution diagram of L-valine/L-leucine in water (orange, ○). 10 mol % 2-propanol/water (red, Δ), 20 mol % 2-propanol/water (blue, *), and 30 mol % 2-propanol/water (green, □) at 298.15 K. The solid lines are calculated with eq 7 using experimental (pseudo-)binary solubility data. Experimental data for water acquired from ref 13.

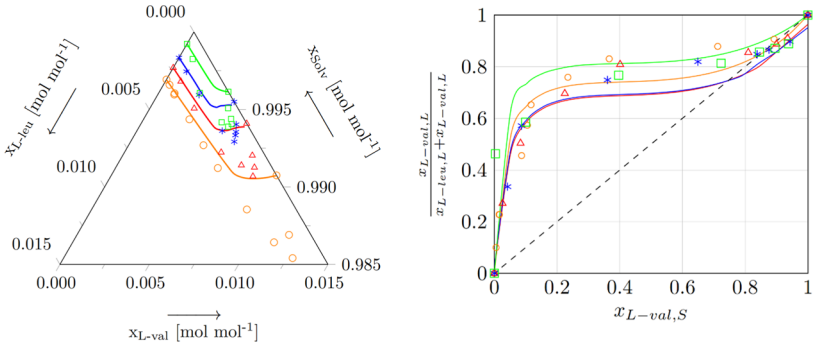

Figure 7. Left: Ternary phase diagram; right: distribution diagram of L-valine/L-leucine in water (orange, ○). 10 mol % acetone/water (red, Δ), 12.5 mol % acetone/water (blue, *), and 15 mol % acetone/water (green, □) at 298.15 K. The solid lines are calculated with eq 7 using experimental (pseudo-)binary solubility data. Experimental data for water acquired from ref 13.

and anchors the model to the experimental data on the edges of the ternary phase diagram. With this approach, the calculation of solid solution solubilities and tie lines remains largely predictive, and therefore, for an initial antisolvent screening, no extensive experiments involving solid solutions need to be performed. For this approach, Figure 5 shows the results for various water/ethanol mixtures in direct comparison to Figure 4, while Figures 6 and 7 show the results in comparison to experimental data sets for water/2-propanol and water/acetone mixtures, respectively.

It can be seen from Figures 4−7 that the model describes a similar behavior for all data sets regarding the solubility, where toward the edges, the model is in good agreement with the experimental data, while the accuracy decreases toward the solubility maximum. Moreover, the solubility decrease is correctly shown and also the alyotropic behavior is observed for all measurements. For systems with ethanol and 2-propanol, the shift of the alyotrope can be described qualitatively and with higher accuracy as the predictive modeling approach using melting data (compare Figures 4 and 7). It should be noted, however, that both approaches result in similar solubilities and tie line behavior for the ternary L-valine/L-leucine/water system. There is a mismatch between the modeling of systems containing acetone and the experimental data to portray the shift of the alyotrope. We assume that this is due to the high volatility of acetone, which leads to slight evaporation during longer equilibration times needed for solid solution solubility measurements. Evaporation leads to an uneven distribution of acetone across various measured samples and results in less reliable data overall. Here, more elaborative experiments at a highly controlled environment are required, which is not that easy. However, if such experiments can be performed, we are confident that the model will be able to depict the correct trends for acetone-containing systems as well.

5. CONCLUSIONS

This work focuses on the measurement and modeling of the solubility and SLE behavior of the amino acids L-valine and L-leucine in various water/antisolvent systems. It is built on a previously proposed modeling approach for continuous solid solution SLE containing a single solvent in the liquid phase.[13] Pure component solubilities of L-leucine were measured and compared with L-valine data from the literature.[7] Acetone showed the lowest solubility for L-valine and the highest for L-leucine. Additionally, acetone exhibited a large change with temperature for the L-leucine solubility, while there was barely a change for the L-valine solubility with temperature. Ethanol and 2-propanol behaved similarly relative to each other, where ethanol showed a higher solubility and a larger temperature dependency of solubility for both solutes. Overall, L-leucine had a higher solubility compared to L-valine in all the considered antisolvents. Thus, L-leucine solubility is less affected by the antisolvent, which leads to an alyotrope shift toward L-valine.

SLEs of systems consisting of various water/2-propanol as well as water/acetone mixtures as the solvent phase were determined experimentally, while SLE data of L-valine and L-leucine mixtures in water and water/ethanol mixtures were taken from previous works.[3,13] 2-Propanol showed a similar antisolvent effect when compared to ethanol, while acetone resulted in a steeper decrease of the solubility.

https://doi.org/10.1021/acs.iecr.2c03122
Ind. Eng. Chem. Res. 2023, 62, 753−761

Two modeling approaches based on melting points and pure solute solubility data were proposed. With both approaches, a description of the solubility decrease was successfully modeled with good agreement toward the pure components. A lower accuracy was achieved at the solubility maximum, likely due to the complex phase behavior imposed by the alyotrope as well as the metastable cocrystal V_3L,[27] which is not regarded in the equilibrium modeling in this work. However, the model based on melting data showed a lower accuracy, and therefore, for an antisolvent screening, the model based on solubility data is recommended. Except for systems in which acetone was used as the antisolvent, a qualitative description of the alyotrope shift with changing solvent composition was predicted. Thus, successful modeling of systems containing acetone requires more detailed elaborate solubility determinations.

Further improvements of the model could consider the effects of pH and temperature. A more extensive antisolvent screening using this model needs to be conducted to obtain an optimal antisolvent for a crystallization-based separation of these amino acids.

■ ASSOCIATED CONTENT

Supporting Information

The Supporting Information is available free of charge at https://pubs.acs.org/doi/10.1021/acs.iecr.2c03122.

Melting data, PC-SAFT, and NRTL parameters acquired from the literature and also several k_{ij} parameters fitted in this work (PDF)

■ AUTHOR INFORMATION

Corresponding Author

Masoud Sadeghi − *Max Planck Institute for Dynamics of Complex Technical Systems, 39106 Magdeburg, Germany;* orcid.org/0000-0003-1911-6225; Phone: +49 391 6110 321; Email: sadeghi@mpi-magdeburg.mpg.de

Authors

Vico Tenberg − *Max Planck Institute for Dynamics of Complex Technical Systems, 39106 Magdeburg, Germany*

Mahsa Hokmabadi − *Max Planck Institute for Dynamics of Complex Technical Systems, 39106 Magdeburg, Germany*

Andreas Seidel-Morgenstern − *Max Planck Institute for Dynamics of Complex Technical Systems, 39106 Magdeburg, Germany*

Heike Lorenz − *Max Planck Institute for Dynamics of Complex Technical Systems, 39106 Magdeburg, Germany;* orcid.org/0000-0001-7608-0092

Complete contact information is available at: https://pubs.acs.org/10.1021/acs.iecr.2c03122

Funding

Open access funded by Max Planck Society.

Notes

The authors declare no competing financial interest.

■ ACKNOWLEDGMENTS

The authors thank Jacqueline Kaufmann and Stefanie Oberländer for their help in HPLC and PXRD measurements as well as Axel Schultheis for his help in the measurement of L-leucine solubilities.

■ LIST OF SYMBOLS

variable	designation, unit
a	activity, [-]
x	mole fraction, [-]
γ	activity coefficient, [-]
T	temperature, [K]
f	fugacity, [Pa]
ΔH_m	melting enthalpy, [J/mol]
ΔC_p	heat capacity difference, [J/mol/K]
m	segment number, [-]
σ	segment diameter, [Å]
u/k	dispersion energy parameter, [K]
ε/k	association energy parameter, [K]
κ	association volume parameter, [-]
k_{ij}	dispersion energy correction parameter, [-]

■ REFERENCES

(1) Kitaigorodsky, A.*Mixed Crystals*; Springer-Verlag: Berlin Heidelberg New York Tokyo, 1984.

(2) Münzberg, S.; Lorenz, H.; Seidel-Morgenstern, A. Multistage Countercurrent Crystallization for the Separation of Solid Solutions. *Chem. Eng. Technol.* **2016**, *39*, 1242.

(3) Tenberg, V.; Sadeghi, M.; Seidel-Morgenstern, A.; Lorenz, H. Bypassing Thermodynamic Limitations in the Crystallization-based Separation of Solid Solutions. *Sep. Purif. Technol.* **2022**, *283*, 120169.

(4) Luk, K. F.; Ko, K. M.; Ng, K. M. Separation and Purification of (-)schisandrin B from Schisandrin B Stereoisomers. *Biochem. Eng. J.* **2008**, *42*, 55.

(5) Lin, S. W.; Ng, K. M.; Wibowo, C. Synthesis of Crystallization Processes for Systems Involving Solid Solutions. *Comput. Chem. Eng.* **2008**, *32*, 956.

(6) Kwok, K. S.; Chan, Y. C.; Ng, K. M.; Wibowo, C. Separation of Fullerenes C60 and C70 Using a Crystallization-based Process. *AIChE J.* **2010**, *56*, 1801.

(7) Zhang, C.; Liu, B.; Wang, X.; Wang, H. Measurement and Correlation of the Solubilities of L-Valine in Water, Ethanol, N, N-Dimethylformamide, Acetone, and Isopropyl Alcohol between (293.15 and 343.15) K. *J. Chem. Eng. Data* **2014**, *59*, 2704.

(8) Held, C.; Cameretti, L.; Sadowski, G. Measuring and Modeling Activity Coefficients in Aqueous Amino-Acid Solutions. *Ind. Eng. Chem. Res.* **2011**, *50*, 131.

(9) Xu, X.; Pinho, S.; Macedo, E. Activity Coefficient and Solubility of Amino Acids in Water by the Modified Wilson Model. *Ind. Eng. Chem. Res.* **2004**, *43*, 3200.

(10) Zhang, C.; Liu, B.; Wang, X.; Wang, H.; Zhang, H. Measurement and Correlation of Solubility of L-Valine in Water + (Ethanol, N, N-Dimethylformamide, Acetone, Isopropyl Alcohol) from 293.15 to 434.15 K. *J. Chem. Eng. Data* **2014**, *59*, 2732.

(11) Bowden, N.; Sanders, J.; Bruins, M. Solubility of the Proteinogenic α-Amino Acids in Water, Ethanol, and Ethanol-Water Mixtures. *J. Chem. Eng. Data* **2018**, *63*, 488.

(12) Ji, P.; Zou, J.; Feng, W. Effect of Alcohol on the Solubility of Amino Acid in Water. *J. Mol. Catal. B: Enzym.* **2009**, *56*, 185.

(13) Sadeghi, M.; Tenberg, V.; Münzberg, S.; Lorenz, H.; Seidel-Morgenstern, A. Phase Equilibria of L-Valine/L-Leucine Solid Solutions. *J. Mol. Liq.* **2021**, *340*, 117315.

(14) Kurosawa, I.; Teja, A. S.; Rousseau, R. W. Solid-Liquid Equilibria in L-Leucine + L-Valine + Water. *Fluid Phase Equilib.* **2005**, *228−229*, 83.

(15) Kurosawa, I.; Teja, A. S.; Rousseau, R. W. Solubility Measurements in the L-Isoleucine + L-Valine + Water System at 298 K. *Ind. Eng. Chem. Res.* **2005**, *44*, 3284.

(16) Daldrup, J.-B. G.; Held, C.; Ruether, F.; Schembecker, G.; Sadowski, G. Measurement and Modeling Solubility of Aqueous Multisolute Amino-Acid Solutions. *Ind. Eng. Chem. Res.* **2010**, *49*, 1395.

(17) Givand, J.; Teja, A. S.; Rousseau, R. W. Effect of Relative Solubility on Amino Acid Crystal Purity. *AIChE J.* **2001**, *47*, 2705.

(18) Givand, J.; Chang, B.-K.; Teja, A. S.; Rousseau, R. W. Distribution of Isomorphic Amino Acids between a Crystal Phase and an Aqueous Solution. *Ind. Eng. Chem. Res.* **2002**, *41*, 1873.
(19) Teja, A. S.; Givand, J.; Rousseau, R. W. Correlation and Prediction of Crystal Solubility and Purity. *AIChE J.* **2002**, *48*, 2629.
(20) Balawejder, M.; Galan, K.; Elsner, M. P.; Seidel-Morgenstern, A.; Piatkowski, W.; Antos, D. Multi-Stage Crystallization for Resolution of Enantiomeric Mixtures in a Solid Solution Forming System. *Chem. Eng. Sci.* **2011**, *66*, 5638.
(21) Gross, J.; Sadowski, G. Perturbed-Chain SAFT: An Equation of State Based on a Perturbation Theory for Chain Molecules. *Ind. Eng. Chem. Res.* **2001**, *40*, 1244.
(22) Smith, J.; Van Ness, H. C.; Abbott, M.; Swihart, M.*Introduction to Chemical Engineering Thermodynamics*, 8th ed.; McGraw-Hill, 2018.
(23) Do, H.; Chua, Y.; Kumar, A.; Pabsch, D.; Hallermann, M.; Zaitsau, D.; Schick, C.; Held, C. Melting Properties of Amino Acids and Their Solubility in Water. *RSC Adv.* **2020**, *10*, 44205.
(24) Prausnitz, J. M.; Lichtenthaler, R. N.; de Azevedo, E. G.*Molecular Thermodynamics of Fluid Phase Equilibria*, 3rd ed.; Wiley-VCH: Weinheim, 1993.
(25) Gross, J.; Sadowski, G. Application of the Perturbed-Chain SAFT Equation of State to Associating Systems. *Ind. Eng. Chem. Res.* **2002**, *41*, 5510.
(26) Chapman, W.; Gubbins, K.; Jackson, G.; Radosz, M. New Reference Equation of State for Associating Liquids. *Ind. Eng. Chem. Res.* **1990**, *29*, 1709.
(27) Isakov, A.; Lorenz, H.; Zolotarev, A., Jr.; Kotelnikova, E. Heteromolecular Compounds in the Binary Systems of Amino Acids with Opposite and Same Chiralities. *CrystEngComm* **2020**, *22*, 986.
(28) Prieto, M. Thermodynamics of Solid Solution-Aqueous Solution Systems. *Rev. Mineral. Geochem.* **2009**, *70*, 47.
(29) Veith, H.; Luebbert, C.; Sadowski, G. Correctly Measuring and Predicting Solubilities of Solvates, Hydrates, and Polymorphs. *Cryst. Growth Des.* **2020**, *20*, 723.
(30) Voges, M.; Fischer, F.; Neuhaus, M.; Sadowski, G.; Held, C. Measuring and Predicting Thermodynamic Limitation of an Alcohol Dehydrogenase Reaction. *Ind. Eng. Chem. Res.* **2017**, *56*, 5535.
(31) Münzberg, S.; Vu, T. G.; Seidel-Morgenstern, A. Generalizing Countercurrent Processes: Distillation and Beyond. *Chem. Ing. Tech.* **2018**, *90*, 1769.

https://doi.org/10.1021/acs.iecr.2c03122
Ind. Eng. Chem. Res. 2023, 62, 753−761